Biophysical Journal, Volume *118*

Supplemental Information

Modulating the Stiffness of the Myosin VI Single α-Helical Domain

C. Ashley Barnes, Yang Shen, Jinfa Ying, and Ad Bax

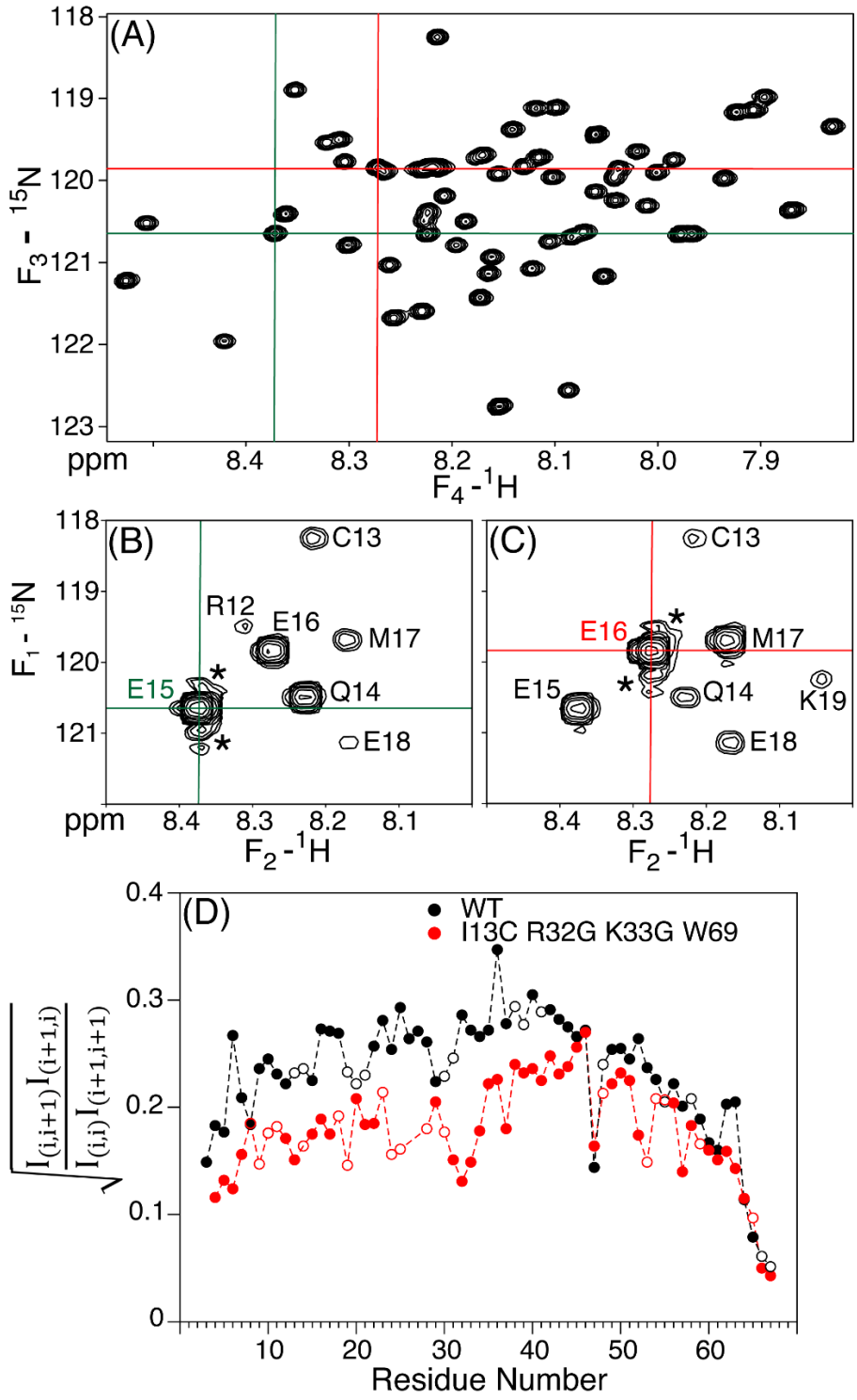

FIGURE S1 4D NOESY data of the I13C/R32G/K33G triple mutant of the myosin VI SAH domain. Experimental parameters are included in Table S5. (A) Small region of the projection of the 4D spectrum onto the (F_3,F_4) TROSY plane, with chemical shift axis calibration adjusted to remove the $^1J_{NH}/2$ component, such that it coincides with the (F_1,F_2) HMQC cross sections shown in (B, C). These HMQC cross sections through the 4D spectrum are orthogonal to the (F_3,F_4)

projection at the positions marked by the green and red cross hairs in (A). Assignments for the diagonal (marked by cross hairs) and cross peaks to adjacent residues are marked by residue numbers. Asterisk mark the truncation artifacts of the intense diagonal resonances. (D) Amide-amide NOE cross peak intensities. Geometric mean of the cross peak over diagonal peak intensity ratios of sequential H^N-H^N NOE interactions observed in the 250 ms mixing time 4D NOESY spectrum of wild type MT (black) and I13C/R32G/K33G triple mutant (red), as a function of residue number. Both 4D spectra were recorded at 900 MHz ^{1}H frequency, 20 °C. Values are only shown for well-resolved peaks whose intensities could be accurately measured. $I_{(i,i)}$ refers to the diagonal intensity of residue *i*, and $I_{(i,i+1)}$ is the sequential cross peak intensity. Experimental uncertainties in the ratios are *ca* 10%; open symbols correspond to interactions where partial overlap of one or both of the diagonal peak made accurate diagonal intensity measurement unreliable. For these cases, diagonal intensity was estimated on the basis of fitting a 4th order polynomial function through the intensities of diagonals whose intensity could be measured unambiguously (Figure S2).

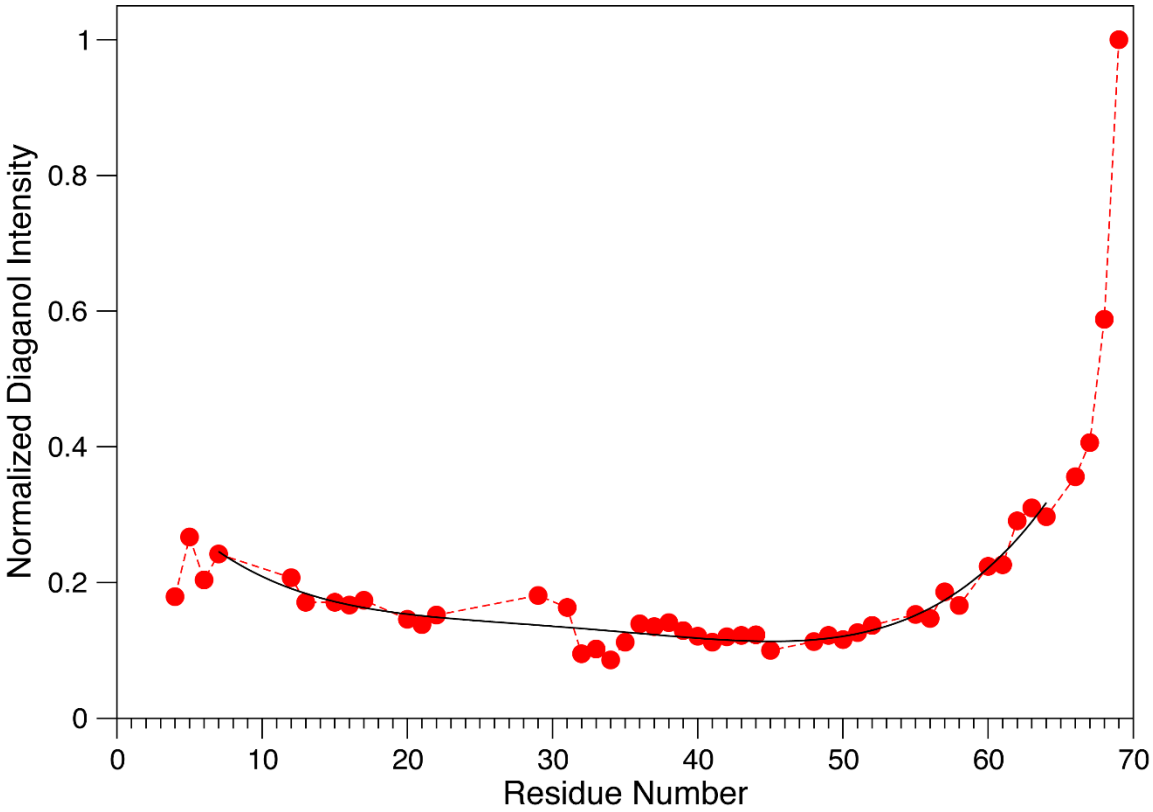

FIGURE S2 Diagonal intensities as a function of residue number for the backbone amides in the 4D NOESY spectrum of the I13C/R32G/K33G mutant of the myosin VI SAH domain. Intensities are normalized such that the highest diagonal intensity is 1. A best fit of the diagonal intensities of residues A7-K63 to a 4th order polynomial is used to estimate diagonal peak intensities that were not fully resolved.

Table S1. Chemical shifts of the native and mutant myosin VI SAH domains, measured in 20 mM sodium phosphate, 2 mM EDTA, 2% D_2O pH=6.3. ^{1}H and ^{15}N chemical shifts are at 20 °C. TCEP (1 mM) was added to the I13C samples.

	WT		**I13C W69**		**I13C R32G W69**		**I13C R32G K33G W69**		**I13C D27H E28H W69**	
Res	^{1}H (ppm)	^{15}N (ppm)	^{1}H (ppm)	^{15}N (ppm)	^{1}H (ppm)	^{15}N (ppm)	^{1}H (ppm)	^{15}N (ppm)	^{1}H (ppm)	^{15}N (ppm)
Q2	8.79	120.01	8.80	119.92	8.80	119.93	8.80	119.94	8.80	119.92
Q3	8.18	119.71	8.16	119.56	8.16	119.57	8.16	119.60	8.16	119.56
E4	8.26	121.70	8.24	121.59	8.24	121.59	8.24	121.59	8.24	121.59
E5	8.54	121.30	8.51	121.12	8.51	121.13	8.51	121.13	8.51	121.12
E6	8.23	121.78	8.22	121.51	8.22	121.51	8.22	121.51	8.22	121.51
A7	8.18	121.00	8.17	121.36	8.17	121.36	8.16	121.36	8.17	121.37
E8	7.89	118.95	7.92	119.13	7.92	119.12	7.92	119.10	7.92	119.14
R9	8.03	121.40	8.05	121.11	8.05	121.11	8.05	121.10	8.06	121.10
L10	8.14	118.02	8.23	119.79	8.22	119.77	8.22	119.77	8.23	119.79
R11	7.99	120.78	7.97	120.59	7.97	120.59	7.97	120.58	7.98	120.61
R12	8.18	119.49	8.32	119.43	8.31	119.44	8.31	119.43	8.32	119.40
I13 (C13)	7.93	120.12	(8.22	118.22)	(8.22	118.21)	(8.21	118.18)	8.21	118.26
Q14	8.01	119.92	8.24	120.40	8.23	120.42	8.22	120.43	8.24	120.41
E15	8.43	120.35	8.38	120.63	8.38	120.61	8.37	120.57	8.38	120.67
E16	8.30	120.27	8.28	119.82	8.27	119.81	8.27	119.77	8.28	119.81
M17	8.37	119.82	8.15	119.56	8.18	119.67	8.16	119.59	8.16	119.56
E18	8.18	121.31	8.17	121.18	8.17	121.16	8.16	121.06	8.16	121.17
K19	8.07	120.34	8.07	120.30	8.06	120.21	8.04	120.17	8.07	120.20
E20	8.03	120.00	8.02	119.98	8.01	119.91	8.00	119.82	8.03	119.92
R21	8.16	121.13	8.15	121.12	8.15	121.13	8.12	121.02	8.16	121.07
K22	8.16	119.07	8.15	119.06	8.14	119.00	8.12	119.04	8.14	119.02
R23	7.96	120.06	7.96	120.03	7.94	119.94	7.93	119.90	7.99	119.93
R24	8.22	119.34	8.21	119.32	8.18	119.40	8.14	119.30	8.22	119.69
E25	8.25	120.27	8.25	120.25	8.25	120.04	8.21	119.75	8.21	120.15
E26	8.34	120.49	8.34	120.48	8.31	120.16	8.22	120.30	8.29	120.32
D27(H27)	8.36	121.07	8.36	121.07	8.31	120.80	8.22	119.76	(8.21	119.08)
E28(H28)	8.24	120.37	8.24	120.38	8.28	120.04	8.22	119.77	(8.32	118.94)
Q29	8.18	118.99	8.18	118.99	8.21	119.77	8.10	119.04	8.42	119.14
R30	8.15	121.12	8.15	121.10	8.14	121.06	8.07	120.54	8.21	120.95
R31	8.18	119.71	8.18	119.69	8.26	119.68	8.22	120.57	8.11	119.76
R32(G32)	8.20	119.43	8.20	119.41	(8.28	107.35)	(8.40	108.49)	8.10	119.88
K33(G33)	8.03	120.87	8.03	120.86	7.98	123.03	(8.31	109.36)	8.06	120.83
E34	8.29	119.59	8.29	119.57	8.31	119.99	8.42	121.89	8.31	119.60

E35	8.22	120.36	8.23	120.36	8.28	120.26	8.49	120.44	8.26	120.10
E36	8.19	121.06	8.19	121.06	8.06	121.03	8.16	120.86	8.19	121.07
E37	8.31	119.84	8.31	119.83	8.25	119.65	8.10	119.88	8.32	119.90
R38	8.07	120.34	8.07	120.27	8.06	120.31	8.03	119.78	8.04	120.21
R39	8.17	119.78	8.17	119.77	8.20	119.76	8.15	119.85	8.19	119.70
M40	8.33	118.77	8.33	118.75	8.36	118.86	8.35	118.83	8.30	118.62
K41	8.07	120.65	8.08	120.61	8.08	120.64	8.10	120.67	8.05	120.64
L42	7.99	120.13	7.99	120.11	7.98	120.13	8.01	120.24	8.01	120.12
E43	8.27	120.90	8.27	120.89	8.26	120.92	8.26	120.96	8.29	120.85
M44	8.32	119.53	8.32	119.53	8.32	119.44	8.32	119.47	8.31	119.59
E45	8.21	120.73	8.21	120.71	8.20	120.70	8.19	120.71	8.21	120.71
A46	8.09	122.50	8.09	122.49	8.09	122.51	8.09	122.50	8.09	122.48
K47	8.03	119.93	8.03	119.94	8.04	119.91	8.04	119.91	8.03	119.91
R48	8.06	120.05	8.06	120.02	8.06	120.05	8.06	120.06	8.05	119.99
K49	8.12	119.76	8.12	119.74	8.12	119.75	8.13	119.77	8.11	119.79
Q50	7.98	119.68	7.98	119.66	7.98	119.66	7.98	119.68	7.98	119.66
E51	8.31	119.70	8.31	119.68	8.30	119.69	8.30	119.69	8.31	119.67
E52	8.19	120.43	8.19	120.43	8.19	120.42	8.19	120.43	8.19	120.43
E53	8.21	120.13	8.21	120.13	8.21	120.13	8.21	120.12	8.20	120.18
E54	8.26	119.83	8.27	119.83	8.27	119.83	8.27	119.83	8.27	119.84
R55	8.07	120.59	8.08	120.62	8.08	120.64	8.08	120.62	8.08	120.61
K56	8.01	119.58	8.02	119.59	8.02	119.59	8.02	119.58	8.02	119.60
K57	7.83	119.30	7.83	119.27	7.83	119.26	7.83	119.26	7.83	119.29
R58	7.89	118.95	7.89	118.90	7.89	118.89	7.89	118.89	7.90	118.92
E59	8.22	119.78	8.22	119.79	8.22	119.78	8.22	119.76	8.23	119.80
D60	8.35	120.28	8.37	120.34	8.37	120.34	8.36	120.34	8.37	120.34
D61	8.28	120.62	8.30	120.71	8.30	120.72	8.30	120.72	8.30	120.71
E62	8.10	119.64	8.11	119.63	8.11	119.63	8.11	119.63	8.11	119.65
K63	7.90	119.18	7.91	119.08	7.90	119.07	7.90	119.07	7.91	119.09
R64	7.89	120.44	7.87	120.30	7.87	120.30	7.87	120.29	7.87	120.30
I65	8.02	120.95	7.98	120.59	7.97	120.59	7.97	120.58	7.98	120.61
Q66	8.28	123.61	8.15	122.70	8.15	122.70	8.15	122.69	8.16	122.70
A67	8.23	125.85	8.09	124.45	8.09	124.46	8.09	124.45	8.09	124.45
E68	7.95	125.34	8.06	119.37	8.06	119.37	8.06	119.37	8.06	119.37
W69			7.62	126.25	7.62	126.25	7.62	126.25	7.62	126.25

Table S2. TROSY ^{15}N transverse relaxation rates ($R_{2,TR}$) of the Ψ-WT and mutant myosin-VI SAH domains in 20 mM sodium phosphate, 2 mM EDTA, 1 mM TCEP, 2% D_2O pH=6.3, 20 °C, measured at 900 MHz ^1H frequency. $R_{2,TR}$ are in inverse seconds and were determined from fitting ^{15}N Hahn-echo decays.

	WT	**I13C/W69**	**I13C/R32G W69**	**I13C/R32G K33G/W69**
	$R_{2,TR}$	$R_{2,TR}$	$R_{2,TR}$	$R_{2,TR}$
E4	4.6	3.6	3.7	3.1
E5	4.6	3.9	3.7	3.1
E6	4.6	3.9	3.9	3.1
A7	5.0	4.5	4.2	3.6
E8		4.1	3.8	3.2
R9	4.5	4.1	4.0	3.2
L10	4.6			
R11	4.6			
R12	4.8	4.6	4.3	3.4
I13(C13)	4.5	(4.9)	(4.5)	(3.6)
Q14	4.8	4.6	4.5	3.6
E15	4.8	4.6	4.4	3.5
E16	4.9	4.9	4.5	3.6
M17	4.9		4.4	
E18	4.9	4.8	4.4	3.4
K19		5.2	4.8	3.4
E20	4.9	4.9	4.7	3.6
R21			4.5	3.5
K22	5.0	4.9	4.6	3.8
R23	5.1	5.1	4.6	3.7
R24	5.3	5.4	4.7	3.9
E25	5.2	5.1	4.9	
E26	5.3		4.8	
D27	5.4	5.3	4.9	3.7
E28	5.3	5.4	4.8	
Q29	5.3	5.2		3.7
R30			4.9	3.6
R31	5.5	5.0		3.7
R32(G32)	5.4	5.2	(5.5)	(4.2)
K33(G33)	5.2	5.0	5.1	(3.7)
E34	5.5	5.2	5.3	4.0
E35	5.3	5.2	5.2	3.9
E36	5.2	5.3	4.8	3.9
E37	5.3	5.2	5.0	3.9
R38		5.0	5.1	4.1
R39		5.5	5.0	4.1

M40	5.3	5.1	4.9	3.9
K41				4.0
L42	5.4	5.3	5.0	4.1
E43	5.3	5.3	5.0	3.9
M44	5.4	5.2	5.0	4.1
E45	5.1	5.0	4.9	4.0
A46	5.4	5.1	5.2	4.4
K47	5.0	5.1	4.9	4.1
R48	5.1	5.0	4.9	4.1
K49	5.1	4.9	4.9	3.8
E50	5.0	4.7	4.6	4.0
E51	5.0	5.1	4.9	4.0
E52	4.8	4.9	4.6	4.0
E53	4.8	4.8	4.5	4.0
E54	4.9	4.7	4.6	4.1
R55				3.9
K56	4.6	4.5	4.5	3.8
K57	4.6	4.6	4.5	3.9
R58		4.6	4.7	3.9
E59	4.5	4.3	4.3	
D60	3.9	3.9	4.0	3.3
D61	3.8	3.6	3.7	3.3
E62	3.6	3.4	3.5	3.0
K63		3.5	3.5	3.1
R64	3.3	2.9	2.9	2.7
I65	2.7		2.8	
Q66	3.1	2.9	2.9	2.7
A67	3.1	2.4	2.5	2.4

Table S3. Hydrogen exchange rates (s^{-1}) of the pseudo WT (E68W), I13C E68W, I13C R32G W69, and I13C R32G K33G W69 MT domains in 20 mM sodium phosphate, 2 mM EDTA, 1 mM TCEP, 2% D_2O at 20 °C and 30 °C.

Residue	**E68W**	**I13C/W68**	**I13C/R32G/W69**		**I13C/R32G/K33G/W69**	
	20 °C pH 7.50	20 °C pH 7.18	20 °C pH 7.51	30 °C pH 7.51[a]	20 °C pH 7.37	30 °C pH 7.37[a]
E4	17	8.7	18	50	14	38
E5	7.5	3.8	8.1	22	5.9	17
E6	6.7	3.3	6.8	21	5.4	17
A7	3.0	1.7	3.6	12	2.7	9.3
E8		1.0	2.2	8.5	1.7	6.5
R9	0.96	0.71	1.6	7.2	1.2	5.6
L10	0.59					
R11	0.60	0.73	1.9	7.6	1.4	5.9
R12	0.75	1.5	2.2	17	2.8	14
C13	0.49	3.3	7.2	33	5.5	25
Q14	0.59	4.1	9.5		7.1	
E15	0.57	1.6	3.1	11	2.4	8.7
E16	0.53	0.75	1.5	5.4	1.2	4.7
M17	0.55		1.4		1.1	5.1
E18	0.78	0.85	1.8	7.8	1.6	6.8
K19		0.46	1.2	4.1	1.1	5.7
E20	0.67	0.45	1.0	4.7	1.1	5.5
R21		0.41	1.9	6.4	1.6	8.1
K22	0.84	0.48	1.6	8.4	2.4	12
R23	0.84	0.51	1.5	8.6	2.3	12
R24	1.1	0.68	2.1	6.0	2.9	15
E25	1.0	0.62	1.7	7.8		3.7
E26	0.85	0.44	1.2	8.8		5.4
D27	1.0	0.49	1.7	5.0	1.8	5.7
E28	0.82	0.42	1.6			6.4
Q29	0.77	0.38	1.5	3.2	3.4	12
R30		0.36	2.4	3.9	4.6	19
R31	0.74		3.7	15	11	34
R32(G32)	0.77	0.37	(10)	(34)	(21)	(50)
K33(G33)	0.86	0.45	7.8	32	(17)	(50)
E34	0.63	0.26	4.2	12	17	50
E35	0.49	0.27	2.3	6.8	8.5	24
E36	0.36	0.16	1.1		2.7	8.2
E37	0.34	0.15	1.1		1.6	5.6
R38		0.20	0.9		1.7	7.3
R39	0.56	0.36	1.5	5.0	1.8	8.0
M40	0.72	0.37	1.0	5.7	1.9	9.2
K41			1.2	6.3	1.8	9.2
L42	0.72	0.35	0.74	3.5	1.0	4.5

E43	0.90	0.37	0.96	4.6	1.1	5.3
M44	1.1	0.63	1.8	6.3	1.5	6.8
E45	1.2	0.53	1.1	5.3	1.2	5.7
A46	1.3	0.52	1.2	6.0	1.2	5.9
K47	1.4	0.58	1.3	6.2	1.2	5.6
R48	1.4	0.69	1.2	5.9	1.1	5.8
K49	2.0	1.0	2.0	9.6	1.6	8.0
Q50	2.3	1.1	2.3		1.8	8.5
E51	1.4	0.69	1.4	6.3	1.0	4.9
E52	1.0	0.45	0.86	3.8	0.63	5.1
E53	0.86	0.38	0.67	3.0	0.51	2.3
E54	1.0	0.47	0.94	5.1	0.72	3.2
R55		0.80	1.2	6.4	1.1	5.3
K56	2.3	1.1	2.2	10	1.6	8.0
K57	2.9	1.3	2.7	11	1.9	8.4
R58		2.2	4.4	21	3.2	14
E59	6.2					
D60	4.0	2.0	3.5	13	2.7	9.7
D61	3.4	1.7	2.9	10	2.2	8.0
E62	3.4	1.5	2.8	8.5	2.1	6.6
K63		2.3	3.7	12	2.8	9.1
R64	11	5.1	9.5	31	6.7	21
I65	6.7	3.2	4.2	15	2.9	11
Q66	20	10	14	50	11	33
A67	26	14	19	49	14	33
E68(W68)	(0.22)	(0.09)	9.5	25	7.2	19
W69			0.14	0.33	0.098	0.23

[a] These pH values were measured at 20 °C and do not include the small decrease in the pH of the solution when the sample temperature is raised to 30 °C.

Table S4. $^{1}D_{NH}$ RDCs measured at 20 °C, 900 MHz, for the W69 I13C-DOTA-M8-Tm tagged variants of the myosin VI SAH domain in 20 mM sodium phosphate, 2 mM EDTA, 2% D_2O pH 5.5, 6.3, and 7.5.

Res	**WT** $^{1}D_{NH}^{20C,pH6.3}$	**R32G** $^{1}D_{NH}^{20C,pH6.3}$	**R32G K33G** $^{1}D_{NH}^{20C,pH6.3}$	**D27H E28H** $^{1}D_{NH}^{20C,pH5.5}$	**D27H E28H** $^{1}D_{NH}^{20C,pH7.5}$
E4	11.6	11.8	13.1	10.0	11.1
E5	22.1	22.0	22.5	20.7	
E6	9.7	11.8	10.1	7.7	9.7
R24	26.1	26.5	24.2	20.3	23.2
E25	30.6	29.2	27.5	23.9	25.6
E26	14.9	15.6	14.6	7.7	12.8
D27(H27)	16.9	19.6	12.8	(9.4)	(13.9)
E28(H28)	27.7	26.1	26.3	(18.3)	(21.7)
Q29	21.2	18.0	15.6	11.4	16.8
R30	12.3	10.7	6.8	4.7	7.9
R31	20.8	14.9	11.4	9.5	
R32(G32)	28.4	(20.4)	(10.7)	14.1	21.1
K33(G33)	15.1	13.0	(3.6)	7.4	12.0
E34	13.8	11.3	4.4	5.8	9.1
E35	24.1	20.5	7.7	12.3	18.4
E36	23.1	19.5	7.1	11.8	18.0
E37	13.0	10.4	3.8	5.4	9.8
R38	14.4	11.4	4.6	5.9	10.8
R39	23.9	19.1	7.4	13.1	17.5
M40	18.4	15.1	5.3	8.5	13.7
K41	10.6	8.2	3.1	2.8	6.5
L42	18.1	14.7	5.5	7.7	13.0
E43	22.3	17.3	7.1	11.7	17.7
M44	12.4	9.6	3.4	4.9	7.5
E45	10.4	7.7	2.4	3.8	6.7
A46	20.3	15.9	5.9	9.7	15.6
K47	18.4	13.4	5.2	8.1	13.3
R48	9.0	8.2	2.7	3.5	5.9
K49	13.2	9.9	3.2	5.2	9.2
Q50	20.9	15.6	6.0		14.9
E51	13.1	10.9	3.4	5.8	9.2
E52	8.0	6.8	1.6	2.0	4.8
E53	15.5	12.5	4.2	7.3	10.3
E54	15.4	13.5	4.7	7.9	13.7
R55	8.5	6.6	2.0	3.3	5.1
K56	8.6	6.8	1.6	6.2	5.8
K57	16.6	13.6	4.0	7.6	12.3
R58	11.6	9.5	2.5	5.3	8.8
E59	5.4	3.9	0.6	1.7	2.8
D60	8.1	6.5	1.6	3.4	6.0
D61	12.6	10.1	2.4	5.7	9.2

E62	5.2	4.4	0.9	1.8	3.4
K63	2.4	2.6	0.3	0.5	1.6
R64	7.9	6.4	1.6	3.8	6.2
I65	2.6	3.4	0.5	2.0	3.3
Q66	-0.3	-0.2	-0.6	-0.6	-0.4
A67	0.2	0.2	-0.6	-0.2	-0.1
E68	2.2	1.7	0.4	1.3	1.7
W69	-0.02	0.008	-0.006	-0.2	0.7

Table S5. Relevant acquisition parameters for the recording of various spectra used in the study of WT and the various mutants of the myosin VI SAH domain.

Exp.	^{15}N, t_1	^{1}H, t_2	^{15}N, t_3	^{1}H, t_4	Sparsity	Mixing	Time	Recycle Delay	NS	^{15}N, F_1	^{1}H, F_2	^{15}N, F_3	^{1}H, F_4
	ms					ms	hours	s		Hz/point			
4D NOESY	30.7	24.5	60.8	162.2	2.1%[a]	250	42.5[a]	3.5	4	3.2	3.1	7.1	13.4
ARTSY	175.4	131.3					3.6	3	4	0.7	1.1		
TROSY-HSQC	109.6	85.2					0.8	2	4	1.4	2.2		
WEX-III TROSY	109.6	121.7					8.0	6	4	0.2	0.4		
^{15}N-TROSY R2	172.8	131.1					19.0	3	8	0.2	0.4		

[a] Sparsity used for the 4D NOESY data of the I13C/R32G/K33G triple mutant of the myosin VI SAH domain. Sparsity of *ca* 1% and correspondingly shorter total measurement time were used for the other constructs.